# Wavelet Representation of Optical System Distortion

Jiri Zahradka David Barina Pavel Zemcik

Faculty of Information Technology
Brno University of Technology
Bozetechova 1/2, Brno
Czech Republic
{izahradka,ibarina,zemcik}@fit.vutbr.cz

## ABSTRACT

A novel method for a representation of the optical system distortion using the discrete wavelet transform is proposed in this paper. Using the presented approach, virtually any complex distortion can be represented only with a small number of wavelet coefficients. Moreover, one can represent the distortion up to the resolution of one pixel or even finer. The experiments shown in the paper suggest that the introduced wavelet interpolation reconstructs distorted data very realistically. The proposed method was evaluated on two scenes comprising a projector and irregular surfaces using dataset of images of various type.

## Keywords

optical distortion, wavelet transform, linear interpolation

## 1 INTRODUCTION

This paper proposes a method for a representation and correction of images geometrically distorted by a complex optical distortion. The distortion may be caused by optical beam refraction or reflection. The refraction can be consequence of passing of the beam through optical lens. An image distorted by reflection is observable for example in an imperfect flat mirror or a curved mirror. In our case, a scene consisting of a projector displaying an image onto an irregular surface is considered as an example.

When the projector displays the image onto an arbitrary surface, the projected image appears distorted. The viewer is represented by a camera. The distortion is caused by passage of the original image through the optical system composed of the projector, surface and camera. The main idea of a distortion correction is to obtain the mapping relation between the captured and the original image. This relation is used for pre-warping of original image which is then displayed by the projector. The mapping relation can be represented as a vector grid [12, 17, 16, 8]. These vectors describe displacement between pixels from original and captured image.

In this paper, we propose a novel method for a representation of such distortion using the discrete wavelet transform. In our approach, the distortion of an optical system is acquired by capturing of projected structured light pattern onto irregular surface. The measured distortion is represented by a rectangular grid of displacement vectors. The grid is then decomposed into the discrete wavelet transform using a suitable wavelet. An approximation of the original field can be computed from only a small number of wavelet coefficients. Moreover, the interpolation of missing displacement vectors can be performed using an inverse transform going beyond the resolution of original vectors.

The presented approach is verified using an optical system consisting of a dataprojector displaying images onto irregular surfaces. The experiments performed on the scenes suggest that the proposed wavelet interpolation can recover the data more precisely compared to naive linear interpolation. This is a consequence of a larger width of a support of well performing CDF 9/7 scaling function in comparison with a support of a linear-interpolating one. The experiments were evaluated on two scenes comprising the projector and irregular surfaces and dataset of six images of various type.

The further sections of this work are organized as follows. The following Related Work section briefly reviews the discrete wavelet transform and methods for modelling of optical distortion. Proposed Method section proposes a novel method of such the representation using the discrete wavelet transform. Using the proposed method, consequent Evaluation section evaluates the approximation for $N$ largest coefficients as well as the interpolation of missing vectors. Finally, Conclusion section closes the paper.

## 2 RELATED WORK

An optical system is a set of optical devices, which affect an optical beam of light passing through. In our case, the optical system consists of a data projector, a projection surface and a digital camera. The camera and the projector affect the optical beam by refraction during passage through their lenses. Optical properties of both devices can be defined by the intrinsic and extrinsic parameters. These parameters describe projective transformation of 3-D points into 2-D image space. The distortions caused by lens shape and position may be described by radial and tangential distortion parameters [7]. Reflection of the optical beam on the projection surface is defined by the laws of reflection [6].

Considering an unknown geometry surface, several methods for a projector distortion correction and a camera-projector automated calibration have been proposed.

R. Raskar [12] proposed a method for irregular surface distortion correction. In his work, a camera captures key points in one image frame of the surface. Mapping relations in these points are calculated utilizing coded projector pattern. Mapping relations in the rest of the projector pixels are computed by bilinear interpolation. In the context of our paper, this method is basically equivalent to interpolation using the linear-interpolating wavelet.

Q. Yuan [17, 16] brought forward a calibration method, which can achieve inner-projector distortion correction and multi-projector registration in a single process. The projector distortion parameters are computed by analysing the coded structured light displayed by the projector using bilinear interpolation. The established mapping relation is stored in relation table which is used for projection source image pre-warping. Also, this method is basically equivalent to using the linear-interpolating wavelet.

Another geometric image calibration method was published by J. Jung [8]. This approach is designed for a handheld data projector to correct geometric distortion of the image projected on non-flat screen surface. The method is using information, such as a slope and curvature extracted from projected pattern key points. The other vertices between key points are obtained by symmetry relation.

D. Cai [1] described non-linear distortion correction surface for continuous curved projective surface. In the approach, a neural network is used to approximate the nonlinear projective transform mapping from camera image to projector image. After the mapping has been established, a transform converter table is constructed from the output of the neural network. The table is utilized for real-time image correction process.

The discrete wavelet transform (DWT) [11] is a mathematical tool which is able to decompose discrete signal into lowpass and highpass frequency components. Such a decomposition can even be performed at several scales. In this paper, we use the CDF 9/7 and 5/3 wavelets [2, 3] which are often used for image compression (e.g., JPEG 2000 standard). Responses of these wavelets can be computed by a convolution with two FIR filters, one with 9 and the other with 7 coefficients in case of CDF 9/7. The transform employing such wavelets can be computed with several successive lifting steps [4, 13]. The resulting coefficients are then divided into two disjoin subbands – approximate and detail coefficients. Another wavelet we employed is the linear-interpolating wavelet (a degenerate instance of the CDF 5/3 in [5]). Considering the lifting scheme of this wavelet, it essentially corresponds to CDF 5/3 wavelet scheme in which an update of the coarse coefficients was omitted.

In case of 2-D transform, the DWT can be realized using separable decomposition scheme [10]. In this scheme, the coefficients are evaluated by successive horizontal and vertical filtering resulting in four disjoin subbands.

The distortion of an optical system can be represented by 2-D equidistant vector field. The DWT of this field is computed separately on its two components ($x$ and $y$). However, more sophisticated wavelet decompositions for vector fields have been developed, e.g. multiwavelets [15]. Note that one wavelet coefficient is thus a vector in context of this article.

Accelerated image resampling algorithms for geometry correction are available. For example, the algorithm in [18] implements essentially same fast resampling as the linear interpolation wavelet used in our paper. The method in [18] can be extended to exploit results of this paper.

## 3 PROPOSED METHOD

In this section, the method of the optical distortion representation using the discrete wavelet transform is presented.

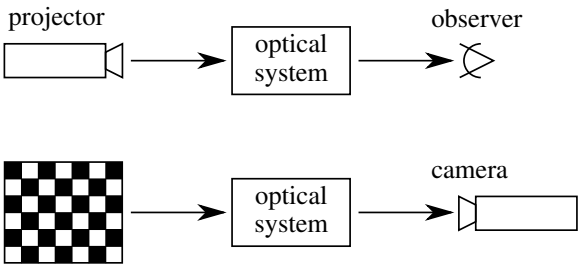


Figure 1: A block diagram of a scene with a human observer (top) which was replaced by a camera and a test pattern (bottom).

While watching the surface on which an original image $O_{(x,y)}$ is projected using a dataprojector, a human observer will see a distorted image

$$D = F(O) \tag{1}$$

where $F$ defines the distortion.

This system is generalized in a top part of Figure 1. Modelling such distortion

$$F_{(x,y)}(X) = X_{(x,y)+f(x,y)} \tag{2}$$

requires measuring of an underlying displacement vector grid $v_{(x,y)}$. The displacement vectors $v_{(x,y)}$ (the mapping relation) can be viewed as

$$f(x,y) = v_{(x,y)} \tag{3}$$

where $f$ is called a distortion mapping.

In more detail, the values from the original image $O$ at coordinate $(x,y)$ are placed into a distorted image $D$ at a coordinate $(x,y)+f(x,y)$. Note that $f$ is a vector-valued function. The set of these displaced values forms $D$.

During the measurement, the distorted test image $D_{(x,y)}$ is obtained by the projection of a test image $O_{(x,y)}$ or series of such images. In our experiments, a classical chessboard image was used. The acquisition of distortion is illustrated in a bottom part of Figure 1. Furthermore, the corrected image

$$C = F(F^{-1}(O)) \tag{4}$$

can be observer by projecting $F^{-1}(O)$. The corresponding correction is given by

$$F^{-1}_{(x,y)}(X) = X_{(x,y)+f^{-1}(x,y)} \tag{5}$$

where $f^{-1}$ is a correction mapping. The similarity between $C_{(x,y)}$ and $O_{(x,y)}$ is measured using several methods in Section Evaluation.

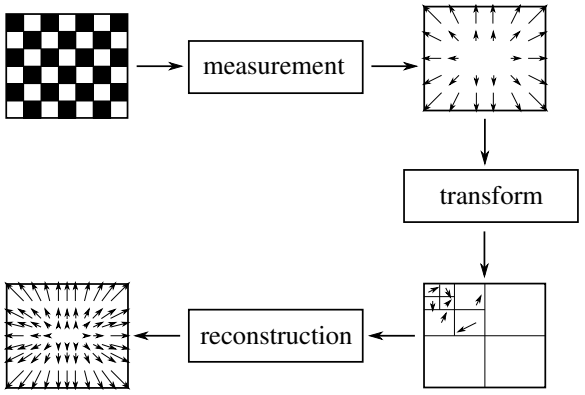


Figure 2: A block diagram of our setup. The acquisition of the vector field is in the upper part.

In this generic form, the distortion $f$ is represented with the 2-D grid of displacement vectors $v_{(x,y)}$. In the scope of this paper, this grid is rectangular and vectors are equidistant. The acquisition was done using a classic chessboard test pattern as shown in Figure 2. The distance between each two vectors is power of two in both of directions. The reason for this is that interpolated vectors should exactly fit pixels in the finest grid resolution.

Considering this grid representation, we propose to store and operate on its discrete wavelet transform

$$\mathrm{W}\, f = \langle f, \psi \rangle \tag{6}$$

where $\psi$ is a wavelet. In terms of this DWT, the coefficients of such transform are approximation $a^j_{x,y}$ and detail $d^j_{x,y}$ vectors for each scale $j$. Now, one can keep only a small number of $N$ largest coefficients to obtain still good approximation of the original distortion field. Moreover, it is easy to interpolate the missing samples using inverse transform $\mathrm{W}^{-1}$. These two opportunities are stated in the bottom part of Figure 2. Both of them are evaluated in the subsequent section.

The transform can be easily computed using a lifting [4] scheme. In the next section, we employed the linear-interpolating wavelet, the CDF 5/3 wavelet and the CDF 9/7 wavelet. The linear-interpolating wavelet corresponds to the CDF 5/3 one with omitted update lifting step. Inverse transform with such wavelet is then equivalent to linear approximation (bi-linear in 2-D case) with the fact that the already known vectors remain unchanged.

## 4 EVALUATION

In this section, the performance of the introduced DWT representation and bi-linear vector interpolation are compared with respect to two different analysis aspects. [1] First task evaluates fidelity of a distortion approximation from only several most significant wavelet coefficients. The second task evaluates interpolation of vector field up to the pixel resolution.

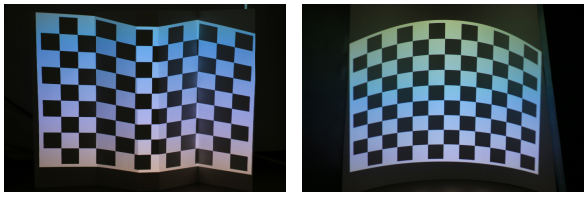

(a) Crumpled (b) Convex

Figure 3: The scenes used in the evaluation. The Crumpled scene contains sharp jumps in the distortion field.

[1] The software implementation is available here: `http://www.fit.vutbr.cz/research/prod/?id=367`

Considering the Convex scene in Figure 3, the evaluation of the interpolation of distortion vector field was performed by keeping only $N$ largest coefficients of DWT. This is known as a non-linear approximation in [11]. As the error of approximation, the Euclidean norm of magnitudes of difference of approximated and original field was used. The result for all of the wavelets can be seen in Figure 4. Approximately above 30 coefficients, CDF 9/7 wavelet overcomes every other. Between 10 and 30 coefficients, CDF 5/3 seems to be better with respect to the Euclidean norm. This range of coefficients is relevant in case someone needs a parameterization using only a very few coefficients.

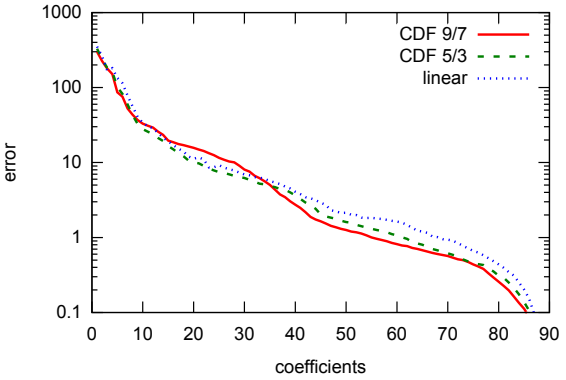


Figure 4: Plot of the Euclidean norm of the error of the vector field approximation using all of the wavelets. The Y axis is in a logarithmic scale.

Evaluating the interpolation of distortion vector field was performed in the following scenario. First, the distortion was estimated using the coarse chessboard pattern projected onto the scene as shown in Figure 2. The sampling interval was $2^6$ pixels in both directions coupled with resolution of $1280 \times 896$ pixels. Then, the vectors were interpolated using the above described CDF wavelet transforms as well as using bi-linear interpolation scheme up to resolution of a reference image. In the following step, this image was deformed (warped) using this dense vector field. The resulting warped image was projected into the scene again giving the corrected image. Now, the corrected and reference images were compared using several metrics described below.

All the evaluations were performed on a dataset consisting of 6 images as shown in Figure 5. Two scenes with different distortions were used as can be seen in Figure 3.

To compare the projection of the corrected images, three quality assessment metrics are used. The first two are the well known PSNR (peak signal-to-noise ratio) and SSIM (structural similarity). The third metric is a simple patch-based correlation. The structural similarity (SSIM) [14] index is a method for measuring the similarity between two images according to human visual perception. The PSNR and SSIM metrics do not consider the geometric distortion that actually occurs in our case.

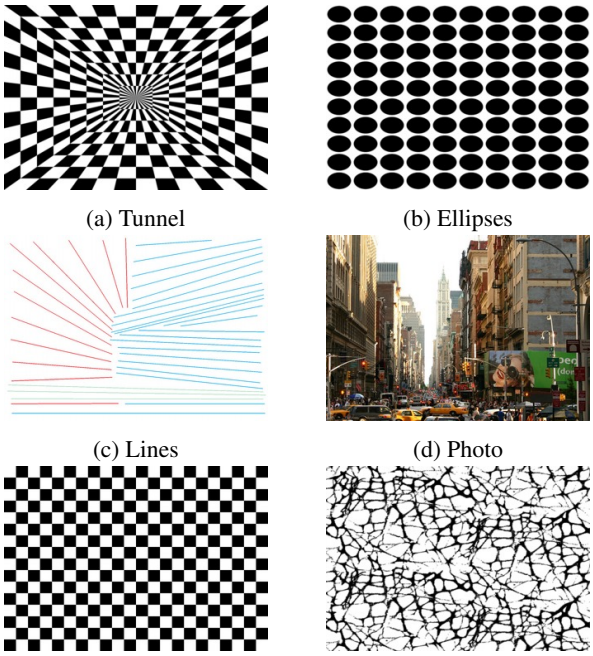

(a) Tunnel (b) Ellipses

(c) Lines (d) Photo

(e) Squares (f) Network

Figure 5: The dataset used in the evaluation.

| image | wavelet | PSNR | SSIM | PBC |
|---|---|---|---|---|
| Tunnel | CDF 9/7 | 10.812 | 0.9910 | **6.366** |
| Tunnel | CDF 5/3 | 10.665 | 0.9907 | 13.161 |
| Tunnel | bi-linear | **10.918** | **0.9913** | 12.589 |
| Ellipses | CDF 9/7 | **12.650** | **0.9938** | **6.134** |
| Ellipses | CDF 5/3 | 12.395 | 0.9934 | 11.554 |
| Ellipses | bi-linear | 12.422 | 0.9935 | 11.607 |
| Lines | CDF 9/7 | 6.936 | 0.9744 | **29.000** |
| Lines | CDF 5/3 | 6.952 | 0.9745 | 35.500 |
| Lines | bi-linear | **6.996** | **0.9748** | 38.500 |
| Photo | CDF 9/7 | **17.466** | **0.9983** | **6.157** |
| Photo | CDF 5/3 | 17.107 | 0.9981 | 11.738 |
| Photo | bi-linear | 16.690 | 0.9978 | 13.855 |
| Squares | CDF 9/7 | 10.667 | 0.9905 | **2.708** |
| Squares | CDF 5/3 | **10.826** | **0.9909** | 8.955 |
| Squares | bi-linear | 10.346 | 0.9896 | 10.663 |
| Network | CDF 9/7 | **8.283** | **0.9841** | **4.451** |
| Network | CDF 5/3 | 8.123 | 0.9833 | 9.348 |
| Network | bi-linear | 7.724 | 0.9814 | 9.696 |

Table 1: Results for scene Crumpled.

Using the patch-based correlation (PBC), a reference image $I^R$ is first decomposed into a set of $P$ patches $\{p_i^R\}_{0<i<P}$, each of a size $L_x \times L_y$. These patches are formed at coordinates $\{c_i^R\}$ around strong image corners and may overlay each other. Corresponding patches $\{p_i^T\}$ with coordinates $\{c_i^T\}$ are then found

(a) reference

(b) CDF 9/7

(c) linear interpolation

Figure 6: Distortion correction performance. From top: a reference image, using CDF 9/7 wavelet, using the linear interpolation. On the latter two images, the location of edges of the original image is highlighted.

| image | wavelet | PSNR | SSIM | PBC |
|---|---|---|---|---|
| Tunnel | CDF 9/7 | 11.784 | 0.9930 | 2.384 |
| Tunnel | CDF 5/3 | **12.054** | **0.9935** | **0.723** |
| Tunnel | bi-linear | 12.020 | 0.9934 | 0.786 |
| Ellipses | CDF 9/7 | 13.471 | 0.9950 | 4.152 |
| Ellipses | CDF 5/3 | **14.081** | **0.9957** | 4.196 |
| Ellipses | bi-linear | 14.016 | 0.9956 | **3.580** |
| Lines | CDF 9/7 | **7.287** | **0.9764** | 23.818 |
| Lines | CDF 5/3 | 6.985 | 0.9747 | 9.308 |
| Lines | bi-linear | 7.172 | 0.9758 | **3.000** |
| Photo | CDF 9/7 | 18.449 | 0.9988 | 2.469 |
| Photo | CDF 5/3 | 17.504 | 0.9982 | **1.975** |
| Photo | bi-linear | **18.896** | **0.9989** | 2.000 |
| Squares | CDF 9/7 | 11.476 | 0.9923 | 0.978 |
| Squares | CDF 5/3 | 11.547 | 0.9924 | **0.966** |
| Squares | bi-linear | **11.989** | **0.9932** | 1.090 |
| Network | CDF 9/7 | 8.494 | 0.9848 | 1.935 |
| Network | CDF 5/3 | 8.445 | 0.9845 | **1.837** |
| Network | bi-linear | **8.544** | **0.9849** | 1.935 |

Table 2: Results for scene Convex.

around the original position in a test image $I^T$. They are identified as maxima of normalized cross-correlations

$$\frac{1}{L_x L_y \sigma_R \sigma_T} \langle (p^R - \bar{p}^R), (p^T - \bar{p}^T) \rangle \tag{7}$$

where $\bar{p}$ is the mean and $\sigma$ is the standard deviation of $p$. Eventually, the metric is defined as an average over squares of Euclidean distances of patch coordinates

$$\frac{1}{P} \sum_i \| c_i^T - c_i^R \|^2 \tag{8}$$

for $0 < i < P$.

The results are summarized in Table 1 and Table 2. We have chosen the patch size of $60 \times 60$ pixels. The patches were weighted by an appropriate Gaussian window. It can be seen that CDF 9/7 wavelet gives best result for Crumpled scene according to PBC metric. In case of Convex scene, the results are unclear. According to PBC metric, the Lines image seems to be unsuitable due to an absence of enough strong corners.

In general, the wavelet interpolation methods generate more smooth vector field in comparison with the linear interpolation. It is a consequence of larger size of the support of wavelet and scaling functions. This property should be more kinder to the human visual system. The statement seems to be confirmed by the results in Table 1 for the Crumpled scene which contains sharp jumps. While this statement is generally valid, still the best results are achieved when the particular wavelet is chosen with respect to the individual scene. Note that PBC metric should be the most significant one because it considers the geometric distortion.

A difference in the execution time of the forward as well as the inverse transform using one of the discussed wavelets should be negligible. The fast algorithms, e.g. [9], limited by the memory access for 2-D discrete wavelet transform exist.

To give a hint on how well the distortion correction performs, Figure 6 shows some images for comparison. The edges of the reference image are highlighted here. Note that CDF 9/7 has a better ability to preserve smooth lines through sharp jumps in the distortion field (Crumpled scene) as compared with the linear interpolation.

## 5 CONCLUSION

We have proposed a method for representation of the geometrical distortion of optical systems using the discrete wavelet transform. This new method allows to approximate the distortion from only a small number of wavelet coefficients. Moreover, it allows to interpolate missing distortion vectors up to a fine scale.

We have evaluated the presented method in scenario in which the image is projected on uneven ground using a dataprojector. In comparison, we have found that the CDF 9/7 wavelet outperforms the bi-linear interpolation when there are sharp jumps in the distortion field. Using a smooth distortion, all the wavelets perform well. In both cases above, the average distance between points in original and observed image is mostly below 3 pixels.

Future research could focus on employing more sophisticated wavelet-like transform in the sense that the basis functions of such transform should fit contours in distortion field. Another area for improvement can be a better measurement of displacement vectors.

## ACKNOWLEDGEMENT

This work has been supported by the EU FP7-ARTEMIS project IMPART (grant no. 316564), the IT4Innovations Centre of Excellence (no. CZ.1.05/1.1.00/02.0070) and the TACR project V3C (no. TE01020415).

## 6 REFERENCES

[1] D. Cai and Y. Dai. A new nonlinear distortion correction approach for camera-projector system. In *WSEAS Int. Conference on Engineering Education*, pages 476–209, 2004. ISBN 960-8457-05-X.

[2] A. Cohen, I. Daubechies, and J.-C. Feauveau. Biorthogonal bases of compactly supported wavelets. *Comm. on Pure and Applied Mathematics*, 45(5):485–560, 1992. ISSN 1097-0312.

[3] I. Daubechies. *Ten lectures on wavelets*. CBMS-NSF regional conference series in applied mathematics. Society for Industrial and Applied Mathematics, 1994. ISBN 9780898712742.

[4] I. Daubechies and W. Sweldens. Factoring wavelet transforms into lifting steps. *Journal of Fourier Analysis and Applications*, 4(3):247–269, 1998. ISSN 1069-5869.

[5] D. Donoho. Interpolating wavelet transforms. *Applied and Comput. Harmonic Analysis*, 1994.

[6] D. Halliday, R. Resnick, and J. Walker. *Fundamentals of Physics*. John Wiley & Sons, 9 edition, 2010. ISBN 978-0470469118.

[7] R. Hartley and A. Zisserman. *Multiple View Geometry in Computer Vision*. Cambridge books online. Cambridge University Press, 2003. ISBN 9781139449144.

[8] J. Jung and J. Cho. Screen adaptive geometric image calibration method for handheld video projector. In *Digest of Technical Papers International Conference on Consumer Electronics*, pages 505–506, 2010. ISBN 978-1-4244-4316-1.

[9] R. Kutil. A single-loop approach to SIMD parallelization of 2-D wavelet lifting. In *Proceedings of the 14th Euromicro International Conference on Parallel, Distributed, and Network-Based Processing (PDP)*, pages 413–420, 2006. ISBN 0-7695-2513-X.

[10] S. Mallat. A theory for multiresolution signal decomposition: the wavelet representation. *IEEE Transactions on Pattern Analysis and Machine Intelligence*, 11(7):674–693, 1989. ISSN 0162-8828.

[11] S. Mallat. *A Wavelet Tour of Signal Processing: The Sparse Way. With contributions from Gabriel Peyré.* Academic Press, 3 edition, 2009. ISBN 9780123743701.

[12] R. Raskar, G. Welch, and H. Fuchs. Seamless projection overlaps using image warping and intensity blending. In *Fourth International Conference on Virtual Systems and Multimedia*, pages 517–521, 1998.

[13] W. Sweldens. The lifting scheme: A custom-design construction of biorthogonal wavelets. *Applied and Computational Harmonic Analysis*, 3 (2):186–200, 1996. ISSN 1063-5203.

[14] Z. Wang, A. Bovik, H. Sheikh, and E. Simoncelli. Image quality assessment: from error visibility to structural similarity. *Image Processing, IEEE Transactions on*, 13(4):600–612, April 2004. ISSN 1057-7149.

[15] M. A. Westenberg and T. Ertl. Denoising 2-D vector fields by vector wavelet thresholding. *Journal of WSCG*, 13(1):33–40, 2005. ISSN 1213-6972.

[16] Q. Yuan and D. Lu. Multi-projector calibration and alignment using flatness analysis for irregular-shape surfaces. In *Advances in Multimedia Information Processing*, volume 5353 of *Lecture Notes in Computer Science*, pages 436–445, 2008. ISBN 978-3-540-89795-8.

[17] Q. Yuan, D. Lu, and Y. He. Scalable arbitrary surrounded surface calibration for multi-projector rendering application. In *International Conference on Virtual Systems and Multimedia*, 2007. ISBN 978-0-9775978-3-3.

[18] P. Zemčík, B. Přibyl, A. Herout, and M. Seeman. Accelerated image resampling for geometry correction. *Journal of Real-Time Image Processing*, 8(4):369–377, 2013. ISSN 1861-8200.